Calcium triggers an intramolecular association of the C2 domains in synaptotagmin

Ricardo A. García*[†], Cameron E. Forde[†], and Hilary Arnold Godwin*[†‡]

*Department of Biochemistry, Molecular Biology, and Cell Biology, 2153 North Campus Drive, Northwestern University, Evanston, IL 60208-3300; and
[†]Department of Chemistry, 2145 Sheridan Road, Northwestern University, Evanston, IL 60208

Synaptotagmin I is a critical component of the synaptic machinery that senses calcium influx and triggers synaptic vesicle fusion and neurotransmitter release. Fluorescence resonance energy transfer studies conducted on synaptotagmin demonstrate that calcium concentrations required for fusion induce a conformational change ($EC_{50} \approx 3$ mM) that brings the two calcium-binding C2 domains in synaptotagmin closer together. Analytical ultracentrifugation studies reveal that synaptotagmin is monomeric under these conditions, indicating that this calcium-triggered association between the C2 domains is intramolecular, rather than intermolecular. These results suggest a mechanism for synaptotagmin function at the presynaptic plasma membrane that involves the self-association of C2 domains.

Calcium mediates neurological signal transduction by triggering the release of neurotransmitter from synaptic vesicles into the synaptic cleft. Substantial progress toward understanding how calcium triggers this response has been made over the last decade, following the identification of a number of proteins involved in docking and fusion of synaptic vesicles (1). Strong evidence points to synaptotagmin I ["synaptotagmin" (syt)] (2) as the protein that senses calcium influx (3). On binding of Ca^{2+}, synaptotagmin binds to the SNARE (soluble *N*-ethylmaleimide-sensitive factor attachment protein receptor) complex (4, 5) on the synaptic cleft and triggers fusion of synaptic vesicles. However, the mechanism by which calcium regulates the fusogenic activity of synaptotagmin has remained elusive.

Synaptotagmin I is anchored to the wall of synaptic vesicles via an N-terminal transmembrane domain and contains two cytosolic calcium-binding C2 domains (C2A and C2B; see Fig. 1*A*).[§] The C2 domains in synaptotagmin I are each highly homologous with the C2 regulatory region of protein kinase C (2), the protein in which the C2 domain was originally identified. C2 domains have subsequently been reported in over 100 proteins in signaling pathways (http://www.expasy.ch/cgi-bin/prosite-search-ac?PS50004) ranging from phospholipid binding and calcium signaling to ubiquitination (6, 7). Despite the pervasive nature of this domain, many fewer structural studies have been reported for proteins containing C2 domains (8–17) than for calcium-binding proteins that contain EF-hand domains (e.g., calmodulin) (18–20). Those structures that have been reported reveal striking differences between the two classes of calcium proteins: whereas EF-hand proteins are entirely α-helical, typically contain a single calcium ion per EF-hand, and have calcium sites that are buried, C2 domains contain a prominent β-barrel and bind multiple calcium ions in a highly exposed surface site.

Synaptotagmin is an unusual calcium sensor even compared with other C2 proteins in that synaptotagmin must respond quickly and reversibly to both low and high influxes of calcium: low calcium concentrations (5–10 μM) trigger phospholipid binding (2, 21–23) and higher calcium concentrations (>200 μM) trigger binding to syntaxin (a member of the SNARE complex) (4). By contrast, calcium-dependent protein kinase C only responds to changes in calcium concentration in the micromolar range, which potentiates phospholipid and membrane binding (24). The two calcium-sensing ranges of synaptotagmin

each confer a different physiological response: whereas phospholipid binding to synaptotagmin results in membrane association and may be critical to docking of synaptic vesicles (23, 25), syntaxin binding is thought to be one of the essential recognition events that allows for calcium-mediated fusion and neurotransmitter release (4, 26). Detailed studies on phospholipid binding to synaptotagmin have revealed that calcium potentiates phospholipid binding by an "electrostatic switch" mechanism: when calcium binds to synaptotagmin, it shields negatively charged residues on the phospholipid binding site and facilitates binding to negatively charged phospholipids (15, 23). By contrast, the mechanism by which calcium regulates the fusogenic activity of synaptotagmin is not well understood, although several mechanisms have been proposed that involve conformational changes, electrostatic switching, and protein dimerization (12, 26–28). Furthermore, the observation that phospholipid and syntaxin binding sites in synaptotagmin are nearly identical (23) raises the intriguing question of how one protein can be tuned to respond to two different calcium-mediated events and provide a unique response to each event.

A clue as to why synaptotagmin exhibits this unusual range of responses to calcium can be gained from a comparison of the domain structure of synaptotagmin with other C2 domain-containing proteins. Whereas protein kinase C and most other C2 proteins contain an isolated C2 domain, synaptotagmins and a small number of other synaptic vesicle proteins such as rabphilin 3A and Doc2 contain two tandem C2 domains, separated by a flexible linker (14, 29, 30). Despite this interesting attribute of synaptotagmins, almost all biophysical studies on synaptotagmins to date have focused on the first C2 domain, C2A. These studies reveal that calcium stabilizes the structure of C2A, but that it does not mediate a large structural change in the isolated domain (7, 8, 12, 17, 31). However, proteolysis studies on the full-length native protein suggest that calcium does induce a conformational change in synaptotagmin (27). Furthermore, binding assays using immobilized synaptotagmin suggest that the second C2 domain, C2B, may play an important role in mediating protein-protein interactions (32–34). Interestingly, a crystal structure of the Mg^{2+}-bound form of the cytosolic C2A-C2B domains of synaptotagmin III revealed that the relative orientation of the two C2 domains was disordered (14). A mechanism that would account for all of these observations that has not been explored previously is that calcium may mediate an intramolec-

---

ular association between the two C2 domains in synaptotagmin. To probe for a calcium-induced conformational change, we have conducted fluorescence resonance energy transfer (FRET) studies on fluorescently labeled synaptotagmin. In addition, we conducted sedimentation equilibrium experiments using analytical ultracentrifugation to determine the association state of synaptotagmin in the presence and absence of calcium.

Materials and Methods

Preparation of Recombinant Fusion Proteins. The cDNAs encoding the cytosolic domain of rat synaptotagmin I (residues 96–421) and its C2B domain (syt249–421) were obtained as glutathione S-transferase fusion constructs from the laboratory of Jonathan Pevsner (Kennedy Krieger Institute). A second C2B construct, syt261–421, was prepared by PCR amplification of the synaptotagmin gene coding for residues 261–421, using PCR primers that contained restriction sites for *Bam*HI (5′) and *Eco*RI (3′). The PCR-derived DNA was digested by *Bam*HI and *Eco*RI endonucleases to create compatible ends for insertion into the glutathione S-transferase expression vector pGEX-PKT (35) at these restriction sites. Successful insertion of the gene was verified by restriction analysis, DNA sequencing, and SDS/PAGE of the protein products. All glutathione S-transferase fusion proteins were overexpressed in *Escherichia coli* BL21/DE3 cells and were purified by affinity chromatography using glutathione-Sepharose beads (Amersham Pharmacia). The glutathione S-transferase moiety was removed by thrombin cleavage on the resin. The proteins were further purified by size-exclusion chromatography using a Superdex 75 column (Amersham Pharmacia). Fractions containing pure protein, as determined by SDS/PAGE, were dialyzed against 10 mM Bis·Tris, 100 mM KCl, and 2 mM EDTA (pH 7.0) and then against 10 mM Bis·Tris and 100 mM KCl (pH 7.0). The concentrations of standardized solutions of synaptotagmin (residues 96–421) and syt249–421 were calibrated by amino acid analysis (Keck Biophysics Facility at Yale University) and were used to calculate the extinction coefficients of these proteins (29,500 $M^{-1}\cdot cm^{-1}$ and 23,500 $M^{-1}\cdot cm^{-1}$, respectively.)

Analytical Ultracentrifugation. Sedimentation equilibrium experiments were conducted by using a Beckman XLA-70 analytical ultracentrifuge. Synaptotagmin (residues 96–421), syt249–421, and syt261–421 were centrifuged at three protein concentrations (10–26 μM) and at multiple speeds (22,000, 27,000, and 32,000 rpm) in an An60 Ti rotor (Beckman) cooled to 4°C. Samples were prepared in buffer (10 mM Bis·Tris/100 mM KCl, pH 7.0) either with no divalent metal added or in the presence of various concentrations of Ca^{2+} (110 μM, 550 μM, 1.1 mM). Attainment of equilibrium was assessed by analysis of difference plots of successive absorbance scans. Data taken at all three speeds and all three protein concentrations were fit simultaneously to single-species and associative models. Data were analyzed by using WINNONLIN3 1.03 (http://spin3.mcb.uconn.edu/) and SEDNTRP 1.01 (ftp://alpha.bbri.org/rasmb/spin/ms_dos/sednterp-philo/) software.

Preparation of Coumarin-Labeled Proteins. The single cysteine (C277) of synaptotagmin, syt249–421, and syt261–421 were labeled with 7-diethylamino-3-(4′-maleimidylphenyl)-4-methylcoumarin ("coumarin") by incubating 50 μM protein in buffer composed of 10 mM Bis·Tris, 100 mM KCl, 500 μM Tris-(2-carboxyethyl)phosphine, and 500 μM 7-diethylamino-3-(4′-maleimidylphenyl)-4-methylcoumarin (pH 7.0) for 10–12 h at 4°C. All tubes and vessels containing the fluorophore were wrapped in aluminum foil to prevent exposure to light. Unreacted 7-diethylamino-3-(4′-maleimidylphenyl)-4-methylcoumarin was removed by extensive dialysis in 10 mM Bis·Tris and 100 mM KCl (pH 7.0). After dialysis, protein concentrations were
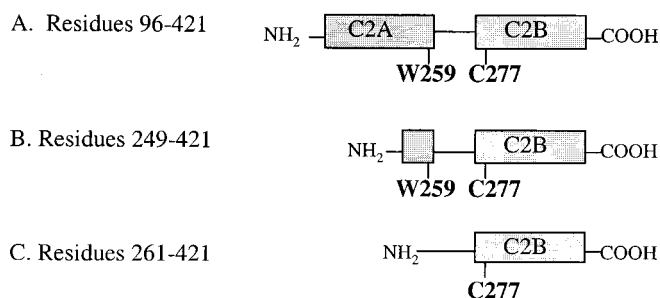
Fig. 1. Schematic representation of synaptotagmin constructs used for FRET studies of metal-dependent C2 domain rearrangement. Shaded boxes denote the regions composing the first and second C2 domains of synaptotagmin (C2A and C2B). The single tryptophan of the C2A domain (W259, energy donor) and the single cysteine of the C2B domain (C277), to which coumarin (energy acceptor) was conjugated, are shown.

determined by using the Bradford Protein Concentration Assay (Bio-Rad).

Fluorescence Resonance Energy Transfer (FRET) Studies of Synaptotagmin. All fluorescence measurements were performed by using an ISS PC1 Photon-Counting Spectrofluorometer equipped with a 300 W xenon arc lamp and a temperature-controlled cuvette holder. Starting conditions were 5 μM protein in 1.5 ml of buffer (10 mM Bis·Tris/100 mM KCl, pH 7.0) in a 1-cm stirred quartz cuvette at 4°C. Slit widths of 1 mm (8-nm bandwidth) were used for the excitation and emission monochromators, and the xenon lamp power supply was set to 18 A. The emission spectra for each sample were measured from 290 to 600 nm by using an excitation wavelength of 280 nm and a cut-on filter at 295 nm to block scattered light from reaching the detector. Each spectrum was taken in 1 nm increments with two integrations per increment. Before starting the metal binding titrations, all protein samples were allowed to equilibrate to 4°C in the fluorometer cuvette chamber for 10 min. The first scan of the emission spectrum (excitation at 280 nm, emission recorded from 290–600 nm) was performed in the absence of metal ion. Titrations were conducted by using an autotitrator, which adds metal solution to the protein in the cuvette; the emission spectrum was recorded after each addition. A total of 45 fluorescence spectra were recorded per experiment. Metal solutions of $BaCl_2$, $CaCl_2$, $MgCl_2$, and $SrCl_2$ were prepared in buffer (10 mM Bis·Tris/100 mM KCl, pH 7.0) at a concentration of 50 mM. At the end of representative titrations, samples were centrifuged, and the concentrations were determined spectrophotometrically to ensure that the protein had not precipitated.

Results

The propensity of rat synaptotagmin I ("synaptotagmin") to undergo a calcium-triggered intramolecular rearrangement was investigated by fluorescence resonance energy transfer (FRET) analysis. FRET studies were performed with the full cytosolic domain of synaptotagmin and two truncated versions containing the C2B domain (syt249–421 and syt261–421; see Fig. 1). The cytosolic domain of synaptotagmin contains a single tryptophan in the C2A domain (W259), two tryptophans in the C2B domain (W390 and W404), and a single cysteine in the C2B domain (C277). The intrinsic fluorescence of W259 in C2A was used as the energy donor. C277 was labeled with coumarin, which absorbs within the region in which W259 emits, and functioned as the energy acceptor. FRET experiments with synaptotagmin were performed with increasing concentrations of Ca^{2+}. Fig. 2*A* shows the fluorescence spectra obtained before and after titrating synaptotagmin with $CaCl_2$. These spectra reveal that the
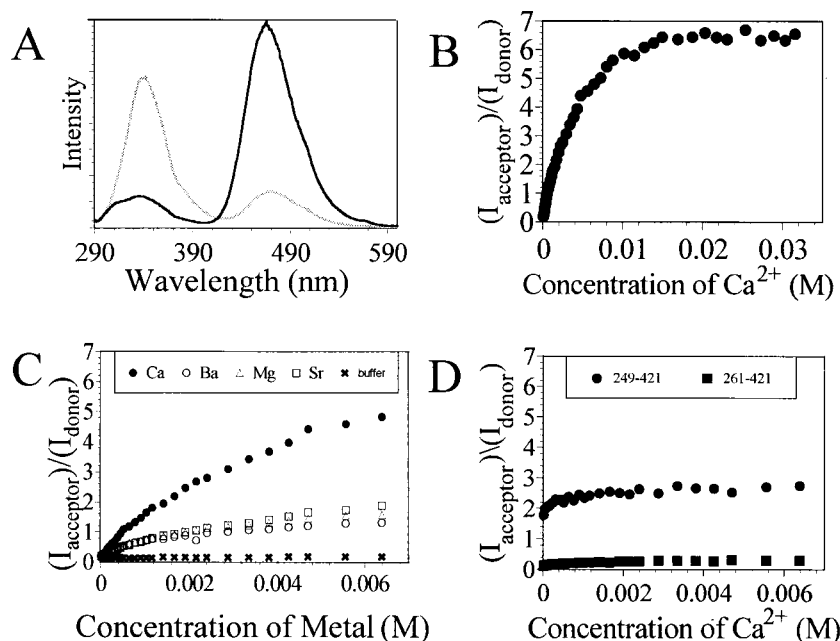
Fig. 2. Fluorescence resonance energy transfer analysis of calcium-induced conformational changes within synaptotagmin. (*A*) Steady-state emission spectra of coumarin-labeled synaptotagmin before (gray line) and after (black line) exposure to ≈32 mM Ca^{2+}. Fluorescence experiments were performed with 5 μM synaptotagmin in 10 mM Bis·Tris and 100 mM KCl (pH 7.0) by using an excitation wavelength of 280 nm. (*B*) Plot showing the ratios of the coumarin/tryptophan peak emission signals for synaptotagmin as a function of Ca^{2+} concentration. (*C*) Comparative plot showing the ratios of the coumarin/tryptophan peak emission signals for synaptotagmin as a function of Ca^{2+}, Ba^{2+}, Mg^{2+}, and Sr^{2+} concentrations relative to buffer only (baseline). (*D*) Comparative plot showing the ratios of the coumarin/tryptophan peak emission signals for syt249–421 and syt261–421 as a function of calcium. Both truncated proteins show calcium-independent behavior; only the protein that contains W259 exhibits significant energy transfer to coumarin.

degree of energy transfer from tryptophan to coumarin increases dramatically after exposure to Ca^{2+}, which implies that the C2 domains are in closer proximity when the protein is in its calcium-bound state (36). The most dramatic changes in fluorescence intensity occur between the calcium concentration range of 33 μM to 10 mM ($EC_{50} \approx 3$ mM; Fig. 2*B*), which is comparable not only to the calcium concentrations required for syntaxin binding (37) but also to the rise in neuronal calcium levels required to evoke exocytosis (38).

To determine whether the metal ion specificity for this conformational change also correlates with that observed previously for syntaxin binding and exocytosis (4), parallel FRET studies were also conducted using Ba^{2+}, Sr^{2+}, and Mg^{2+}. Addition of Ba^{2+}, Sr^{2+}, or Mg^{2+} to labeled synaptotagmin causes an increase in energy transfer from tryptophan to coumarin (Fig. 2*C*). These observations are consistent with a previous report that exposure of synaptotagmin to Ca^{2+}, Ba^{2+}, or Sr^{2+} gives rise to similar proteolytic patterns (27) and that Ba^{2+}, Sr^{2+}, and, to a lesser extent, Mg^{2+}, can potentiate synaptotagmin-syntaxin interactions *in vitro* under some conditions (4). However, these FRET studies also reveal that the extent of energy transfer potentiated by Ba^{2+}, Sr^{2+}, or Mg^{2+} is considerably reduced compared with that seen for Ca^{2+} and/or that the binding of these metal ions to synaptotagmin is considerably weaker (Fig. 2*C*). Thus, these results demonstrate definitively that the conformational response of synaptotagmin to millimolar concentrations of calcium is not identical to that seen for other metal ions. The observation that Sr^{2+} does not evoke the same FRET response as calcium is consistent with the inability of Sr^{2+} to consistently potentiate either syntaxin binding to synaptotagmin I (39) or the fast (evoked) component of neurotransmitter release (40). The parallels between the metal specificity of the global conformational change and that seen for syntaxin binding

and exocytosis support the assertion that the conformational change we observe is involved in triggering exocytosis (39, 40).

In addition to the one tryptophan residue in the C2A domain of synaptotagmin (W259), two other tryptophan residues are present at the end of the C2B domain (W390 and W404) opposite from the calcium binding site. To determine the extent to which these tryptophan residues contribute to the observed energy transfer to the acceptor (coumarin-C277), FRET studies were conducted on two different versions of isolated C2B domain. First, Ca^{2+} titrations were conducted with a truncated version of synaptotagmin (syt261–421; Fig. 1*C*) that contains the entire C2B domain but lacks the putative energy donor, W259. The fluorescence spectra showed only minor changes from the start of the titration to the end and resembled spectra obtained with the entire cytosolic domain of synaptotagmin titrated with buffer (Fig. 2 *C* and *D*). These data reveal that neither energy transfer from W390 nor energy transfer from W404 can account for the dramatic increase in coumarin emission seen for full-length synaptotagmin in the presence of calcium. Ca^{2+} titrations were also conducted with a second truncated version of synaptotagmin (syt249–421; Fig. 1*B*) that contains the C2B domain and a remnant of the C2A domain with the W259 residue, but does not contain the C2A calcium-binding site. The fluorescence spectra for syt249–421 showed virtually complete energy transfer from the start of the titration to the end (Fig. 2*D*), indicating that W259, which is no longer confined within the structure of the C2A domain, is in close proximity to the energy acceptor on the C2B domain. These results demonstrate that W259 on the C2A domain functions as the principal energy donor to the acceptor (coumarin-C277) on the C2B domain.

The C2B domain of synaptotagmin had previously been reported to mediate dimerization of synaptotagmin (33). This raises the question of whether the calcium-dependent change in energy transfer observed for full-length synaptotagmin (Fig. 2 *A*
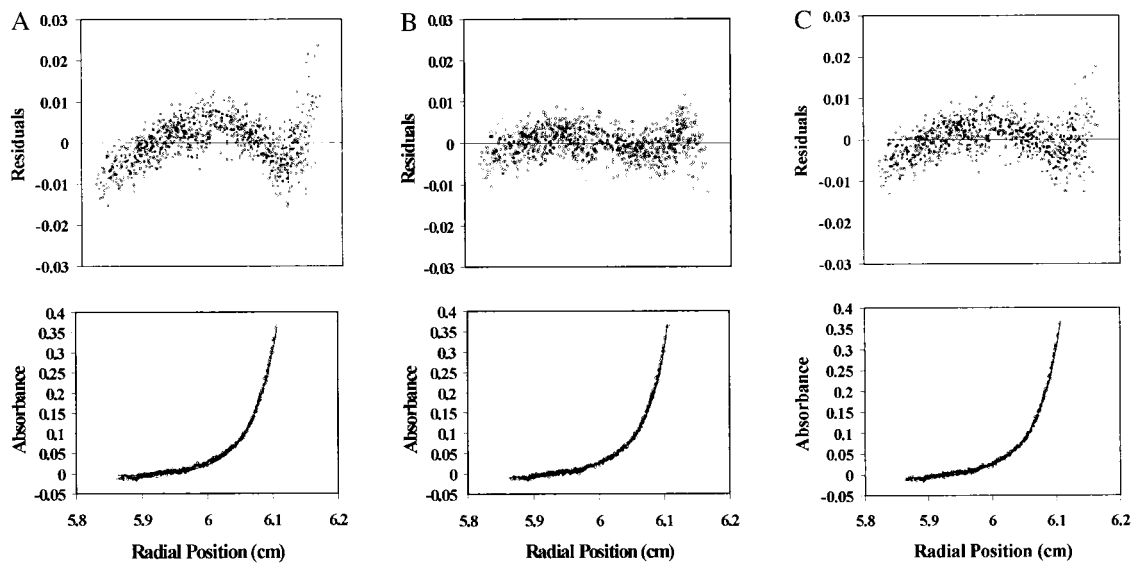
Fig. 3. Sedimentation equilibrium analysis of synaptotagmin. Samples of synaptotagmin (3–10 μM) were centrifuged at multiple speeds (22,000, 27,000, and 32,000 RPM) as described in *Materials and Methods*. For clarity, only the absorbance scans taken at 27,000 RPM are shown. The resulting data from eight absorbance scans taken at 280 nm as a function of radial position and the corresponding fitted curve are shown in the lower panels, and the distribution of residuals are shown in the upper panels. The data were fit simultaneously to the following models: "single ideal species" model (*A*), "single non-ideal" species model (*B*), and "monomer-dimer ideal associative" model (*C*).

and *B*) is attributable to an intermolecular association between synaptotagmin molecules or to an intramolecular association of C2 domains. To address this issue, we performed a series of sedimentation equilibrium experiments using analytical ultracentrifugation on the full cytosolic domain of synaptotagmin and on the two truncated proteins in the presence and absence of calcium. Sedimentation equilibrium results obtained with the full cytosolic domain of synaptotagmin (30,504–38,897 Da) (Fig. 3) are consistent with the calculated molecular mass of the polypeptide (37,187 Da), indicating that the protein is predominantly monomeric, even when exposed to calcium (Table 1). The best fit to these data are obtained by using a single non-ideal species model (Fig. 3*B*). Use of an associative model does not improve the quality of the fit (Fig. 3*C*) and yields a dissociation constant ($\geq$ 100 mM) for syt-syt interactions that is too high to be physiologically relevant (Table 1). It is therefore unlikely that the increase in energy transfer involves an obligatory dimerization event on calcium-binding. Similarly, both of the truncated proteins appear as monomers in solution (syt261–421, 17,124–20,811 Da; syt249–421, 15,971–19,232 Da) under these conditions (Table 2).

Discussion

The data provided here show that calcium binding to synaptotagmin causes a dramatic alteration in the relative orientation of the C2A and C2B domains. The marked increase in coumarin emission on exposure of synaptotagmin to increasing concentrations of Ca^{2+} suggests that calcium binding causes the C2A and C2B domains to come closer together. Sedimentation equilibrium studies reveal that synaptotagmin is monomeric, even in the presence of high calcium. Taken together, these studies provide evidence that calcium activates synaptotagmin by inducing a conformational change that causes an intramolecular association of C2A and C2B. Given that the EC_{50} of this response for Ca^{2+} (approximately 3 mM) is similar to the Ca^{2+} requirements for syntaxin binding and synaptic vesicle fusion (37, 38), we propose that this conformational switch is necessary for its interactions with the SNARE complex and exocytosis. These data are also consistent with the earlier proposal by Südhof and

coworkers that calcium mediates synaptotagmin-syntaxin binding via an "electrostatic switch" mechanism (12, 26). When Ca^{2+} binds to the C2A domain, the electrostatic potential of the Ca^{2+}-binding pocket is switched from negative to positive,

Table 1. Results of sedimentation equilibrium studies on synaptotagmin using analytical ultracentrifugation (actual molecular mass of synaptotagmin is 37,187 Da)

Single ideal species model		
Sample	Molecular mass, Da	Standard deviation of fit
apo-syt	46,922	5.09×10^{-3}
syt + 110 μM Ca^{2+}	44,537	5.30×10^{-3}
syt + 550 μM Ca^{2+}	46,617	4.79×10^{-3}
syt + 1.1 mM Ca^{2+}	49,243	4.86×10^{-3}

Single non-ideal species model		
Sample	Molecular mass, Da	Standard deviation of fit
apo-syt	36,113	3.46×10^{-3}
syt + 110 μM Ca^{2+}	30,504	3.52×10^{-3}
syt + 550 μM Ca^{2+}	33,897	3.04×10^{-3}
syt + 1.1 mM Ca^{2+}	38,897	3.93×10^{-3}

Monomer-dimer ideal associative model			
Sample	Molecular mass, Da	K_d	Standard deviation of fit
apo-syt	34,009	>100 mM	4.09×10^{-3}
syt + 110 μM Ca^{2+}	31,975	>100 mM	4.34×10^{-3}
syt + 550 μM Ca^{2+}	34,347	>100 mM	4.08×10^{-3}
syt + 1.1 mM Ca^{2+}	33,015	$\approx$100 mM	4.41×10^{-3}

The best fit to the data is obtained by using a single non-ideal species model. Use of an associative model does not improve the quality of the fit and yields a K_d for synaptotagmin-synaptotagmin interactions ($\geq$100 mM) that is too high to be physiologically relevant.

Table 2. Sedimentation equilibrium results for syt249–421 (molecular mass of 19,853 Da) and syt261–421 (molecular mass of 18,395 Da)

Single ideal species model		
Sample	Molecular mass, Da	Standard deviation of fit
apo-syt249–421	26,608	6.36×10^{-3}
syt249–421 + 110 μM Ca^{2+}	24,435	5.36×10^{-3}
syt249–421 + 550 μM Ca^{2+}	26,108	7.23×10^{-3}
syt249–421 + 1.1 mM Ca^{2+}	26,273	4.43×10^{-3}

Single non-ideal species model		
Sample	Molecular mass, Da	Standard deviation of fit
apo-syt249–421	15,971	2.54×10^{-3}
syt249–421 + 110 μM Ca^{2+}	16,734	3.01×10^{-3}
syt249–421 + 550 μM Ca^{2+}	15,202	2.78×10^{-3}
syt249–421 + 1.1 mM Ca^{2+}	19,232	3.24×10^{-3}

Single ideal species model		
Sample	Molecular mass, Da	Standard deviation of fit
apo-syt261–421	19,969	6.20×10^{-3}
syt261–421 + 110 μM Ca^{2+}	19,186	6.66×10^{-3}
syt261–421 + 550 μM Ca^{2+}	21,637	3.68×10^{-3}
syt261–421 + 1.1 mM Ca^{2+}	21,902	6.30×10^{-3}

Single non-ideal species model		
Sample	Molecular mass, Da	Standard deviation of fit
apo-syt261–421	17,124	3.63×10^{-3}
syt261–421 + 110 μM Ca^{2+}	18,204	3.81×10^{-3}
syt261–421 + 550 μM Ca^{2+}	17,756	3.43×10^{-3}
syt261–421 + 1.1 mM Ca^{2+}	20,811	6.31×10^{-3}

Both truncated versions of the protein are best fit using a single non-ideal species model and are monomeric in solution.

allowing synaptotagmin to bind to the negatively charged binding region of syntaxin and to mediate vesicle fusion.

The suggestion that calcium mediates a conformational change in synaptotagmin via an electrostatic mechanism is also supported by the recent crystal structure of the cytosolic domain of synaptotagmin III in the presence of magnesium (14). In this structure, the two individual C2 domains each are well ordered and have magnesium bound. However, the linker between C2A and C2B is completely disordered, and hence the relative orientations of the two domains cannot be determined. Furthermore, the authors see no evidence for extensive interdomain

contacts, suggesting that this divalent metal ion does not cause a structural rearrangement that allows for direct contact between the two domains. Rather, based on our studies, we suggest that synaptotagmin populates an ensemble of conformations, each of which has the same C2 domain structure, but with a different relative orientation of C2A and C2B. A large change in the electrostatics will occur on calcium binding, which could be responsible for the reorientation of the two domains relative to each other (Fig. 4). The net charge on the two domains could be very different in the calcium-bound state: C2A is expected to be positively charged but it is not clear what the net charge on C2B would be. In the crystal structure of synaptotagmin III, three metal ions are bound to C2A but only one is bound to C2B (14). More detailed studies of the metal-binding and electrostatic properties of both domains are needed to determine definitively whether an electrostatic switching mechanism is responsible for the conformational change reported herein.

Several other questions remain unanswered and merit further investigation. First, does the protein simply "relax" to a preferred state on binding of calcium (i.e., on release of repulsion)? Our studies on syt249–421 suggest that this may be the case: the truncated protein, which contains W259 but not the negatively charged calcium binding residues from C2A, exhibits moderate energy transfer that is calcium-independent. Alternatively, it is possible that the calcium binding sites in the two loops are both positively charged in the calcium-bound state and that repulsion of these two loops on calcium binding causes the other ends of the two domains to move closer together because the two domains are tethered. We are currently conducting parallel studies on full-length proteins with altered metal binding sites to further probe this issue. In addition, time-resolved experiments will provide critical insights into the distribution of conformations that are populated in both the calcium-free and calcium-bound states. From a bioinorganic chemistry perspective, the question of why other divalent metal ions do not fully mimic calcium is also of critical interest. Furthermore, the possibility that synaptotagmin may be a molecular target for lead—and that this interaction may account in part for lead's neurotoxicity (C. Bouton, L. P. Frelin, C.E.F., H.A.G., and J. Pevsner, unpublished work)—raises the intriguing question of whether lead is able to induce this conformational change. Clearly, more extensive studies on the metal-binding properties of synaptotagmin, and the relationship between metal binding and the conformational change reported herein, are warranted.

What might be the functional importance of the global conformational changes associated with synaptotagmin during the late stages of vesicle fusion and neurotransmitter release? To date, tandem C2 domains have only been identified in a small subset of known C2-domain containing proteins, each of which is a synaptic vesicle-associated protein (e.g., synaptotagmin family members, rabphilin 3A, and Doc2). This suggests that the global conformational change we report here may be specific to
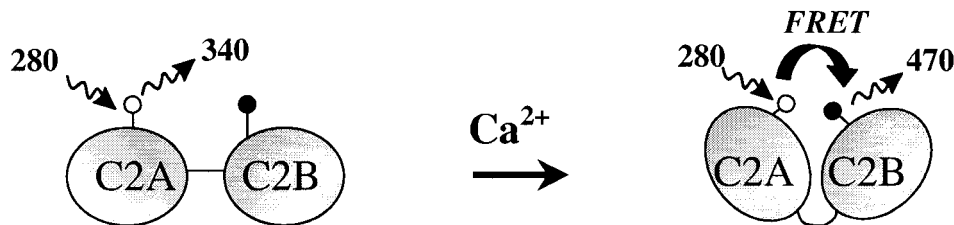
Fig. 4. Schematic depiction of the calcium-triggered activation of synaptotagmin. In the absence of calcium, the two C2 domains of synaptotagmin, C2A and C2B, are far apart and very little energy transfer is observed. Donor (W259) is represented by the white circle on C2A; acceptor (coumarin) is represented by the black circle on C2B. On calcium binding, C2A and C2B undergo an intramolecular association, bringing W259 on C2A and coumarin on C2B closer together, and the extent of energy transfer increases dramatically.

this important class of proteins for their function in exocytosis and endocytosis. In the case of synaptotagmin, it is possible that any global changes in synaptotagmin's conformation could be relayed to the SNARE complex and to the phospholipid membranes (4, 26, 41). Such changes in conformation might be readily "sensed" at the membrane-anchored ends of synaptotagmin and the SNARE proteins. The strain in the membrane at these protein anchor sites could deform the lipid bilayers and promote lipid mixing between the presynaptic plasma membrane and the synaptic vesicle membrane. A similar fusion mechanism involving only the SNARE proteins has been proposed in which the joining of the two membranes and the subsequent fusion event are driven by SNARE complex formation (5). Membrane fusion mediated by the influenza viral protein hemagglutinin is triggered by a change in the tertiary structure of the protein (42). It is believed that the conformational change in hemagglutinin mediates fusion by destabilizing both the viral membrane and the target membrane. Therefore, the conformational changes observed with synaptotagmin could serve as a fusion-catalyst during synaptic transmission. Clearly, in the long run, studies must be conducted on membrane-bound synaptotagmin to determine whether its properties mirror those reported herein for the cytosolic region of the protein.

1. Rizo, J. & Sudhof, T. C. (1998) *Nat. Struct. Biol.* **5,** 839–842.
2. Perin, M. S., Fried, V. A., Mignery, G. A., Jahn, R. & Sudhof, T. C. (1990) *Nature (London)* **345,** 260–263.
3. Kelly, R. B. (1995) *Curr. Biol.* **5,** 257–259.
4. Chapman, E. R., Hanson, P. I., An, S. & Jahn, R. (1995) *J. Biol. Chem.* **270,** 23667–23671.
5. Sutton, R. B., Fasshauer, D., Jahn, R. & Brunger, A. T. (1998) *Nature (London)* **395,** 347–353.
6. Nalefski, E. A. & Falke, J. J. (1996) *Protein Sci.* **5,** 2375–2390.
7. Rizo, J. & Sudhof, T. C. (1998) *J. Biol. Chem.* **273,** 15879–15882.
8. Sutton, R. B., Davletov, B. A., Berghuis, A. M., Sudhof, T. C. & Sprang, S. R. (1995) *Cell* **80,** 929–938.
9. Essen, L. O., Perisic, O., Cheung, R., Katan, M. & Williams, R. L. (1996) *Nature (London)* **380,** 595–602.
10. Essen, L. O., Perisic, O., Lynch, D. E., Katan, M. & Williams, R. L. (1997) *Biochemistry* **36,** 2753–2762.
11. Perisic, O., Fong, S., Lynch, D. E., Bycroft, M. & Williams, R. L. (1998) *J. Biol. Chem.* **273,** 1596–1604.
12. Shao, X., Fernandez, I., Sudhof, T. C. & Rizo, J. (1998) *Biochemistry* **37,** 16106–16115.
13. Xu, G.-Y., McDonagh, T., Yu, H.-A., Nalefski, E. A., Clark, J. D. & Cumming, D. A. (1998) *J. Mol. Biol.* **280,** 485–500.
14. Sutton, R. B., Ernst, J. A. & Brunger, A. T. (1999) *J. Cell Biol.* **147,** 589–598.
15. Chae, Y. K., Abildgaard, F., Chapman, E. R. & Markley, J. L. (1998) *J. Biol. Chem.* **273,** 25659–25663.
16. Davletov, B., Perisic, O. & Williams, R. L. (1998) *J. Biol. Chem.* **273,** 19093–19096.
17. Ubach, J., Zhang, X., Shao, X., Sudhof, T. C. & Rizo, J. (1998) *EMBO J.* **17,** 3921–3930.
18. Ikura, M. (1996) *Trends Biochem. Sci.* **21,** 14–17.
19. Kawasaki, H., Nakayama, S. & Kretsinger, R. H. (1998) *Biometals* **11,** 277–295.
20. Nelson, M. R. & Chazin, W. J. (1998) *Biometals* **11,** 297–318.
21. Brose, N., Petrenko, A. G., Sudhof, T. C. & Jahn, R. (1992) *Science* **256,** 1021–1025.
22. Davletov, B. A. & Sudhof, T. C. (1993) *J. Biol. Chem.* **268,** 26386–26390.
23. Zhang, X., Rizo, J. & Sudhof, T. C. (1998) *Biochemistry* **37,** 12395–12403.
24. Medkova, M. & Cho, W. (1998) *J. Biol. Chem.* **273,** 17544–17552.
25. Chapman, E. R. & Jahn, R. (1994) *J. Biol. Chem.* **269,** 5735–5741.
26. Shao, X., Li, C., Fernandez, I., Zhang, X., Sudhof, T. C. & Rizo, J. (1997) *Neuron* **18,** 133–142.
27. Davletov, B. A. & Sudhof, T. C. (1994) *J. Biol. Chem.* **269,** 28547–28550.
28. Damer, S. K. & Creutz, C. E. (1996) *J. Neurochem.* **67,** 1661–1668.
29. Shirataki, H., Kaibuchi, K., Sakoda, T., Kishida, S., Yamaguchi, T., Wada, K., Miyazaki, M. & Takai, Y. (1993) *Mol. Cell. Biol.* **13,** 2061–2068.
30. Orita, S., Sasaki, T., Naito, A., Komuro, R., Ohtsuka, T., Maeda, M., Suzuki, H., Igarashi, H. & Takai, Y. (1995) *Biochem. Biophys. Res. Commun.* **206,** 439–448.
31. Shao, X., Davletov, B. A., Sutton, R. B., Sudhof, T. C. & Rizo, J. (1996) *Science* **273,** 248–251.
32. Kee, Y. & Scheller, R. H. (1996) *J. Neurosci.* **16,** 1975–1981.
33. Chapman, E. R., An, S., Edwardson, J. M. & Jahn, R. (1996) *J. Biol. Chem.* **271,** 5844–5849.
34. Chapman, E. R., Desai, R. C., Davis, A. F. & Tornehl, C. K. (1998) *J. Biol. Chem.* **273,** 32966–32972.
35. Sehgal, B. U., Dunn, R., Hicke, L. & Godwin, H. A. (2000) *Anal Biochem.*, in press.
36. Stryer, L. & Haugland, R. P. (1967) *Proc. Natl. Acad. Sci. USA* **58,** 719–726.
37. Fernandez, I., Ubach, J., Dulubova, I., Zhang, X., Sudhof, T. C. & Rizo, J. (1998) *Cell* **94,** 841–849.
38. Llinas, R., Sugimori, M. & Silver, R. B. (1992) *Science* **256,** 677–679.
39. Li, C., Davletov, B. A. & Sudhof, T. C. (1995) *J. Biol. Chem.* **270,** 24898–24902.
40. Goda, Y. & Stevens, C. F. (1994) *Proc. Natl. Acad. Sci. USA* **91,** 12942–12946.
41. Schiavo, G., Stenbeck, G., Rothman, J. E. & Sollner, T. H. (1997) *Proc. Natl. Acad. Sci. USA* **94,** 997–1001.
42. White, J. M. (1992) *Science* **258,** 917–924.